
Bayesian Optimization with Hidden Constraints via Latent Decision Models

Wenqian Xing
Stanford University

Jungho Lee
Carnegie Mellon University

Chong Liu
University of Chicago

Shixiang Zhu
Carnegie Mellon University

Abstract

Bayesian optimization (BO) has emerged as a potent tool for addressing intricate decision-making challenges, especially in public policy domains such as police districting. However, its broader application in public policymaking is hindered by the complexity of defining feasible regions and the high-dimensionality of decisions. This paper introduces the Hidden-Constrained Latent Space Bayesian Optimization (HC-LSBO), a novel BO method integrated with a latent decision model. This approach leverages a variational autoencoder to learn the distribution of feasible decisions, enabling a two-way mapping between the original decision space and a lower-dimensional latent space. By doing so, HC-LSBO captures the nuances of hidden constraints inherent in public policymaking, allowing for optimization in the latent space while evaluating objectives in the original space. We validate our method through numerical experiments on both synthetic and real data sets, with a specific focus on large-scale police districting problems in Atlanta, Georgia. Our results reveal that HC-LSBO offers notable improvements in performance and efficiency compared to the baselines.

1 Introduction

In recent years, Bayesian optimization (BO) has been proven successful in solving complex decision-making problems, showcasing its ability to optimize intricate black-box objective functions that are typically difficult to analyze explicitly [Shahriari et al., 2015]. This positions BO as a powerful tool for designing public policy, such as police districting [Zhu et al., 2020, Zhu et al., 2022], site selection for emergency service systems [Xing and Hua, 2022], hazard assessment



(a) Pre-2019 (b) Post-2019 (c) Infeasible

Figure 1: An illustrative example showing the difficult-to-define constraints using three districting plans for the Atlanta Police Department (APD). Gray lines represent the basic geographical units patrolled by the police, red lines outline the districting plans, and dashed blue lines highlight the changes made to the pre-2019 plan. (a) and (b) are feasible plans implemented by the APD pre and post 2019. (c) shows an infeasible plan that was turned down by the APD because it overlooked traffic constraints and inadvertently cut off access to some highways with its zone boundaries.

[Xie et al., 2021] and public healthcare policymaking [Chandak et al., 2020]. Policymakers tackling such optimization problems often need to work through complex human systems, where the evaluation of potential decisions can be analytically implicit and resource-intensive.

However, the broader application prospects of BO in public policymaking are hampered due to two major hurdles: (1) Defining the feasible region or setting clear constraints for decisions is inherently complicated for real human systems. Policymakers often encounter a myriad of both explicit and implicit rules when making an optimal decision, adding a significant layer of complexity to the optimization process. For instance, in police districting, police departments often organize their patrol forces by dividing the geographical region of a city into multiple patrol areas called zones. Their goal is to search for the optimal districting plan that minimizes the workload variance across zones [Larson, 1974, Larson and Odoni, 1981, Zhu et al., 2020, Zhu et al., 2022]. As shown in Figure 1, a well-conceived plan necessitates each zone

to adhere to certain shape constraints (*e.g.*, contiguity and compactness) that are analytically challenging to formulate [Shirabe, 2009], while also taking socio-economic or political considerations into account (*e.g.*, ensuring fair access to public facilities). This creates a web of *hidden constraints* [Choi et al., 2000, Audet et al., 2020] that are elusive to define clearly, making the assessment of feasible region nearly as expensive as evaluating the objective itself [Gardner et al., 2014]. (2) The decisions for public policy are usually high-dimensional, presenting a significant computational hurdle to utilizing traditional BO methods [Luong et al., 2019, Wan et al., 2021, Binois and Wycoff, 2022]. For example, the districting problem can be formulated by mixed-integer programming, grappling with hundreds or even thousands of decision variables even for medium-sized service systems [Zhu et al., 2020, Zhu et al., 2022].

Despite the difficulty in formulating constraints for decisions in public policymaking, the rich repository of historical decisions adopted by the practitioners, combined with the increasingly easier access to human systems [van Veenstra and Kotterink, 2017, Yu et al., 2021], offer a wealth of feasible decision samples. Collecting these samples might involve seeking guidance from official public entities on decision feasibility or generating decisions grounded in domain expertise, bypassing the need to understand the explicit form of the constraints. These readily available feasible decisions harbor implicit knowledge that adeptly captures the dynamics of hidden constraints, providing a unique opportunity to skillfully address these issues. This inspires us to develop a *latent decision model* that maps the feasible region in the original space to a lower-dimensional latent space and encapsulates the key pattern of these hidden constraints. As a result, the majority of existing BO methods can be directly applied to solve the original optimization problem in this latent space without constraints.

In this paper, we aim to solve Hidden-Constrained Black-Box Optimization (HCBBO) problems. In these problems, *the constraints are not analytically defined and the feasibility of a given random decision is also indeterminable*. Our primary asset is a set of observed feasible decisions. To this end, we propose a novel Bayesian optimization method integrated with a latent decision model, which we refer to as Hidden-Constrained Latent Space Bayesian Optimization (HC-LSBO), designed to solve high-dimensional HCBBO problems. The latent decision model leverages a variational autoencoder (VAE) [Doersch, 2016] to capture the underlying distribution of feasible decisions in a data-driven manner. This model acts as

an additional surrogate alongside the Gaussian process (GP) in BO, aiding the decision transition between the original and latent spaces. As a result, while objective evaluations are performed in the original space, the search for new decisions takes place in the latent space. We validate that our proposed algorithm can achieve a no-regret upper bound with a judiciously chosen number of observations in the original space. In addition, we showcase numerical results derived from both synthetic and real data sets. In our real experiments, we apply the proposed method to solve large-scale districting problems for police operation systems in Atlanta, Georgia. The results demonstrate inspiring empirical performance as well as efficiency against the baseline methods. In summary, this paper’s key contributions are:

1. We formulate a new class of optimization problems called Hidden-Constrained Black-Box Optimization (HCBBO), which cannot be readily addressed by the existing BO methods.
2. We propose HC-LSBO algorithm that effectively tackles high-dimensional HCBBO problems.
3. We introduce a latent decision model that facilitates a lower-dimensional, more compact, and unconstrained space for BO algorithms.
4. Our results demonstrate the superior performance of our model against the baseline methods on both synthetic and real data sets, particularly in scenarios with complex hidden constraints.

Related work Black-box optimization, a.k.a. zeroth-order optimization or derivative-free optimization, is a long-standing challenging problem in optimization and machine learning. Existing work either assumes the underlying objective function is drawn from some Gaussian process [Williams and Rasmussen, 2006] or some parametric function class [Dai et al., 2022, Liu and Wang, 2023]. The former one is usually known as Bayesian optimization (BO), with the Gaussian process serving as the predominant surrogate model. BO has been widely used in many applications, including but not limited to neural network hyperparameter tuning [Kandasamy et al., 2020, Turner et al., 2021], material design [Ueno et al., 2016, Zhang et al., 2020], chemical reactions [Guo et al., 2023], and public policy [Xing and Hua, 2022].

In numerous real-world problems, optimization is subject to various types of constraints. Eriksson proposes scalable BO with known constraints in high dimensions [Eriksson and Poloczek, 2021]. Letham explores BO in experiments featuring noisy constraints [Letham et al., 2019]. Gelbart pioneered the concept of BO with unknown constraints [Gelbart et al., 2014], later enhanced by Aria through the ADMM framework

[Ariafar et al., 2019]. Their constraints are unknown due to uncertainty but can be evaluated using probabilistic models. In addition, Choi and Audet study the unrelaxable hidden constraints in a similar way [Choi et al., 2000, Audet et al., 2020], where the feasibility of a decision can be evaluated by another black-box function. In contrast, in our problem, the feasibility of an arbitrary decision is unavailable and we only have access to a set of feasible decision samples.

Building on latent space methodologies, Varol presented a constrained latent variable model integrating prior knowledge [Varol et al., 2012]. Eissman [Eissman et al., 2018] presents a method emphasizing training VAE from labeled data. Deshwal and Doppa focus on combining latent space and structured kernels over combinatorial spaces [Deshwal and Doppa, 2021]. Maus further investigates structured inputs in local spaces [Maus et al., 2022], and Antonova introduces dynamic compression within variational contexts [Antonova et al., 2020]. However, it’s worth noting that none of these studies consider any types of constraints in their methodologies.

Additionally, there is another line of work aiming to solve offline black-box optimization. Char and Chen work on optimization using offline contextual data [Char et al., 2019, Chen et al., 2023]. Krishnamoorthy explores offline black-box optimization through diffusion models [Krishnamoorthy et al., 2023]. Similar to our approach, these studies adopt data-driven methodologies but heavily rely on prior $(x, f(x))$ pairs. In contrast, our approach only requires pre-existing knowledge of feasible x decisions.

2 Preliminaries

Problem setup W.l.o.g., consider a decision space denoted by $\mathcal{X} \subseteq [0, 1]^d$ where 1 can be replaced with any universal constant, which represents a specific region of a d -dimensional real space. Suppose there exists a black-box objective function, $f : \mathcal{X} \mapsto \mathbb{R}$, that can be evaluated, albeit at a substantial cost. Assume we can obtain a noisy observation of $f(x)$, denoted as $\hat{f}(x) = f(x) + \epsilon$, where ϵ follows a σ -sub-Gaussian noise distribution. The goal is to solve the following optimization problem:

$$\begin{aligned} \min_{x \in \mathcal{X}} f(x) \\ \text{s.t. } h(x) \leq 0, \forall h \in \mathcal{H}. \end{aligned}$$

where \mathcal{H} denotes a set of constraints.

Assuming we lack direct access to the analytical expression of $h \in \mathcal{H}$, these constraints are either impossible to explicitly formulate or computationally impractical. Now suppose we have n observations of feasible decisions, denoted by $X = \{x_1, x_2, \dots, x_n\} \subset \mathcal{X}$.

These observations are subject to the hidden constraints and are uniformly distributed in the feasible decision space $\mathcal{F} = \{x \in \mathcal{X} \mid h(x) \leq 0 \text{ for all } h \in \mathcal{H}\}$. In practice, these samples can be sourced by consulting human systems or generated based on the domain knowledge. For example, new feasible districting plans in Figure 1 can be created by first randomly altering the assignments of border regions and then checking their feasibility through police consultations.

Bayesian optimization (BO) The BO algorithms prove especially valuable in scenarios where the evaluation of the objective function is costly or time-consuming, or when the gradient is unavailable. This approach revolves around constructing a *surrogate model* of the objective function and subsequently employing an *acquisition function* based on this surrogate model to determine the next solution for evaluation. For the minimization problem, a popular choice of surrogate model is the Gaussian process with the lower confidence bound (LCB) [Srinivas et al., 2009] serving as the acquisition function.

The Gaussian process (GP) in the space \mathcal{X} , denoted by $\text{GP}(\mu, k; \mathcal{X})$, is specified by a mean function $\mu(x)$ and a kernel function $k(x, x')$, which indicates the covariance between the two arbitrary decisions x and x' . The GP captures the joint distribution of all the evaluated decisions and their observed objective function values. We reference the standard normal distribution with zero mean and an identity matrix I as its variance by $\mathcal{N}(0, I)$, and let $Y = \{\hat{f}(x) \mid x \in X\}$ represent the corresponding set of objective function values. For a new decision \tilde{x} , the joint distribution of Y and its objective function value \tilde{y} of \tilde{x} is

$$\begin{bmatrix} Y \\ \tilde{y} \end{bmatrix} \sim \mathcal{N} \left(\mu \left(\begin{bmatrix} X \\ \tilde{x} \end{bmatrix} \right), \begin{bmatrix} K(X, X) + \sigma^2 I & K(X, \tilde{x}) \\ K(X, \tilde{x})^\top & k(\tilde{x}, \tilde{x}) \end{bmatrix} \right),$$

where σ^2 represent the variance of the observed noise ϵ . Here $K(X, X) = (k(x, x'))_{x, x' \in X}$ denotes the covariance matrix between the previously evaluated decisions and $K(X, \tilde{x}) = (k(x, \tilde{x}))_{x \in X}$ denotes the covariance vector between the previously evaluated decisions and the new decision.

3 Proposed method

The main idea of our method is to perform Bayesian optimization within a low-dimensional feasible latent space denoted as $\mathcal{Z} \subseteq \mathbb{R}^{d'}$ with $d' \ll d$, rather than the constrained original decision space. The latent space \mathcal{Z} is learned using a VAE, which leverages the set of observed feasible decisions X as the training data.

To be specific, we train the VAE model by maximizing the evidence lower bound $\mathcal{L}_{\text{ELBO}}(X)$. This VAE model enables a two-way mapping of decisions between

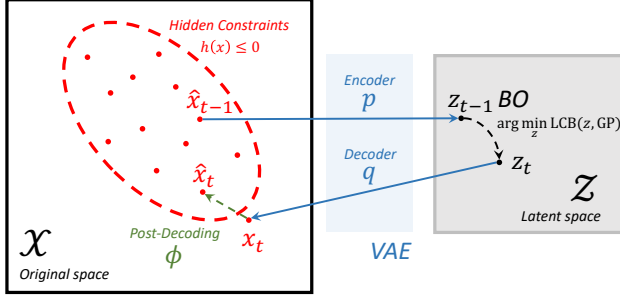


Figure 2: An illustration of the HC-LSBO algorithm. Red dots indicate observed feasible decisions, while the dotted circle shows the feasible region we can’t directly access. For each iteration, the feasible decision \hat{x}_{t-1} is mapped to the latent space using an encoder p . A new decision z_t is then chosen in the latent space by minimizing the lower confidence bound (LCB). Lastly, this new decision z_t is mapped back to the original space using decoder q and translated to the closest feasible decision \hat{x}_t via the post-decoding process ϕ .

the original and latent spaces, achieved through an *encoder* p and a *decoder* q . Given an initial set of random feasible decisions from X denoted as X_0 , we first obtain their objective values denoted as $Y_0 = \{\hat{f}(x) \mid x \in X_0\}$. These decisions are then encoded to the latent space using p , represented by $Z_0 \subset \mathcal{Z}$. As illustrated by Figure 2, for each iteration t , our BO algorithm is performed as follows: (1) Train a surrogate model $\text{GP}(\mu, k; \mathcal{Z})$ using the latent decisions Z_{t-1} and their observed values Y_{t-1} . (2) Search for the next latent decision candidate z_t by sampling m latent decisions and selecting the one with the lowest LCB value. (3) Decode the newly identified latent decision z_t to the original space using q , yielding a new decision x_t . (4) Substitute x_t with \hat{x}_t using a *post-decoding* process ϕ which finds the nearest feasible decision of x_t in the set X . The BO algorithm iterates a total of T times. The proposed method is summarized in Algorithm 1. In the remainder of this section, we explain each component of our proposed method at length.

3.1 Latent decision model

To address the challenge of hidden constraints in HCBBO problems, we introduce a latent decision model based on a VAE in our framework. The reason is two-fold: (1) To encode the underlying feasible region in the original decision space into a compact, continuous, and constraint-free latent space. (2) To condense the dimensionality of the original problem, making BO more feasible in the latent space. Figure 3 provides a visualization of solution paths of our algorithm in both the original (2D) and latent (1D) spaces for solving the same optimization problem. We observe that BO can navigate within an unconstrained

Algorithm 1: HC-LSBO

Input: Feasible decisions X ; Objective function \hat{f} ; Hyper-parameters m, T .
 Train an VAE (p, q) by maximizing $\mathcal{L}_{\text{ELBO}}(X)$;
 Randomly select $X_0 \subseteq X$;
 Evaluate $Y_0 = \{\hat{f}(x) \mid x \in X_0\}$;
 $Z_0 \leftarrow p(X_0)$; // Encode X_0
for $t \leftarrow 1$ **to** T **do**
 Train $\text{GP}(\mu, k; \mathcal{Z})$ using (Z_{t-1}, Y_{t-1}) ;
 $\hat{Z} \sim \mathcal{N}(0, I)$; // Sample m latent decisions
 $z_t = \text{argmin}_{z \in \hat{Z}} \text{LCB}(z, \text{GP})$;
 $x_t \leftarrow q(z_t)$; // Decoding
 $\hat{x}_t \leftarrow \phi(x_t)$; // Post-decoding
 $X_t \leftarrow X_{t-1} \cup \{\hat{x}_t\}$, $Z_t \leftarrow Z_{t-1} \cup \{z_t\}$;
 $Y_t \leftarrow Y_{t-1} \cup \{\hat{f}(\hat{x}_t)\}$;
end
return $x^* = \text{argmin}_{x \in X_T} \hat{f}(x)$

latent space, which offers a simpler structure in the objective function, thanks to the latent decision model.

Suppose there exists a joint distribution between the decision $x \in \mathcal{X} \subseteq \mathbb{R}^d$ and a latent variable $z \in \mathcal{Z} \subseteq \mathbb{R}^{d'}$, with $d' \ll d$. We represent the posterior distribution $q(z|x)$ and the conditional distribution $p(x|z)$ using neural networks [Pineiro Cinelli et al., 2021]. Since it is intractable to directly optimize the marginal maximum likelihood of x , the evidence lower bound (ELBO) [Jordan et al., 1999] of the log-likelihood is derived as follows

$$\mathcal{L}_{\text{ELBO}}(x) = \mathbb{E}_{q(z|x)} [\log p(x|z)] - \eta \text{D}_{\text{KL}}(q(z|x) \parallel \varphi(z)), \quad (1)$$

where $\varphi(z)$ represents the prior distribution of z and η is a hyperparameter that modulates the penalization ratio. Here we assume the prior of z follows a standard Gaussian distribution $\mathcal{N}(0, I)$. The first term in (1) can be considered as the reconstruction error between the input and reconstructed decisions, and the second term is the Kullback–Leibler (KL) divergence between the Gaussian prior of the latent variable z and the learned posterior $q(z|x)$. For the sake of notational simplicity, we use p and q to represent the encoder and decoder functions, respectively, throughout this paper. The complete derivation of (1) and implementation details can be found in Appendix A.

Post-decoding process To ensure the decoded decision $x \in \mathcal{X}$ is subject to the hidden constraints, we introduce a post-decoding process in addition to the decoder, denoted by $\phi : \mathcal{X} \mapsto \mathcal{F}$. This function projects x to the closest feasible decision $\hat{x} \in \mathcal{F}$.

However, the presence of the hidden constraints \mathcal{H} prevents us from achieving an exact projection. As

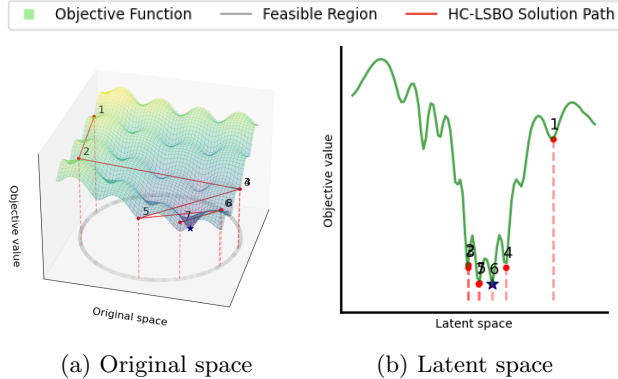


Figure 3: Solution paths of the same optimization problem suggested by our HC-LSBO algorithm in the (a) original and (b) latent spaces, respectively. The objective in this illustrative example is to minimize the Ackley function subject to a “hidden” constraint (a circle) in a 2D decision space.

a workaround, we search within the observational set X , rather than the unattainable feasible region \mathcal{F} , and find a feasible decision $\hat{x} \in X$ that is the closest to the decoded decision x as an approximate. The distance between any two decisions is measured by the Euclidean norm $\|\cdot\|_2$. Formally,

$$\phi(x) = \operatorname{argmin}_{\hat{x} \in X} \|\hat{x} - x\|_2.$$

3.2 Surrogate model

Now we define the following *indirect objective function* $g(\cdot)$ which maps from $\mathcal{Z} \mapsto \mathbb{R}$:

$$g(z) = f(\phi(q(z))).$$

The indirect objective function measures the objective value of the latent variable via the decoder q and the post-decoding process ϕ . Since the objective function f is a black-box function in nature, the indirect objective function g is also a black-box function.

We use a GP as our surrogate model of the indirect objective function g , denoted by $\text{GP}(\mu, k; \mathcal{Z})$. In our problem, the mean function can be written as $\mu(z) = \mathbb{E}[g(z)]$. In addition, we adopt the Matérn kernel [Seeger, 2004] as the kernel function $k(z, z') = \mathbb{E}[(g(z) - \mu(z))(g(z') - \mu(z'))]$, which is widely-used in BO literature. The main advantage of the GP as a surrogate model is that it can produce estimates of the mean evaluation and variance of a new latent variable, which can be used to model uncertainty and confidence levels for the acquisition function described in the following. Note that the latent variable z is assumed to follow a Gaussian prior in the latent decision model, which aligns with the assumption of the GP model that the observed latent variables Z follow the multivariate Gaussian distribution.

Acquisition function In the BO methods, the acquisition function is used to suggest the next evaluating candidate. Our approach adopts the lower confidence bound (LCB) as the acquisition function to choose the next latent variable z candidate to be decoded and evaluated. This function contains both the mean $\mu(z)$ of the GP as the explicit exploitation term and the standard deviation $\sigma(z)$ of the GP as the exploration term:

$$\text{LCB}(z, \text{GP}) = \mu(z) - \sqrt{\beta} \sigma(z),$$

where β is a trade-off parameter.

To search for new latent decisions for evaluation, our method first draws m independent latent samples, denoted as \hat{Z} , from the standard Gaussian prior $z \sim \mathcal{N}(0, I)$. Then we select the decision with the lowest LCB value, denoted by z_t , for decoding and evaluation by the objective function \hat{f} in the t -th iteration.

4 Theoretical analysis

In this section, we provide theoretical analysis for Algorithm 1. Recall that we denote $p: \mathcal{X} \mapsto \mathcal{Z}$ as the encoder function and $q: \mathcal{Z} \mapsto \mathcal{X}$ as the decoder function. The $g(z) = f(\phi(q(z))) : \mathcal{Z} \mapsto \mathbb{R}$ denotes the objective function w.r.t. \mathcal{Z} . Further, we define z_t as the output of the GP-LCB algorithm and x_t as its associated data point in \mathcal{X} via q ; define \hat{x}_t as the data point after post-decoding processing of x_t and \hat{z}_t as its associated data point in \mathcal{Z} via p .

We use cumulative regret to evaluate the performance of our algorithm which is defined as follows.

$$R_T = \sum_{i=1}^T f(\hat{x}_i) - f(x_*).$$

And the expected cumulative regret:

$$\mathbb{E}[R_T] = \mathbb{E} \left[\sum_{i=1}^T f(\hat{x}_i) - f(x_*) \right],$$

where the expectation is taken over all randomness, including random noise and random sampling over n observation data points.

Here we list two assumptions that will be used. The first assumption is made on the property of encoder and decoder.

Assumption 1 (Forward and backward mapping). *The encoder and decoder are inverse operations of each other, i.e.,*

$$x = q(p(x)) \quad \text{and} \quad z = p(q(z)), \quad \forall x \in \mathcal{X}, z \in \mathcal{Z}.$$

Also, we assume the distance between any two points in \mathcal{Z} can be upper bounded by their distance in \mathcal{X} , i.e.,

$$\|p(x) - p(x')\|_2 \leq C_p \|x - x'\|_2, \quad \forall x, x' \in \mathcal{X}.$$

where C_p is a universal constant.

The next assumption is the standard Gaussian process assumption for Bayesian optimization.

Assumption 2 ([Srinivas et al., 2010]). *Function $g : \mathcal{Z} \mapsto \mathbb{R}$ is drawn from some Gaussian Process and it is C_g -differentiable, i.e.,*

$$|g(z) - g(z')| \leq C_g \|z - z'\|_2, \quad \forall z, z' \in \mathcal{Z},$$

where C_g is a universal constant.

Now we are ready to state our main theoretical result.

Theorem 3. *Suppose Assumptions 1 and 2 hold. After running T iterations, the expected cumulative regret of Algorithm 1 satisfies that*

$$\mathbb{E}[R_T] = \tilde{O}(\sqrt{T\gamma_T} + \sqrt{dn}^{-\frac{1}{d+1}}T),$$

where γ_T is the maximum information gain, depending on choice of kernel used in algorithm and n is number of observation data points.

Remark 4. *This upper bound has two terms. The first term follows from GP-UCB [Srinivas et al., 2010] where the maximum information gain depends on the choice of kernel used in the algorithm. The second term is the regret term incurred by the post-processing function ϕ . Although it is linear in T , it can still be sublinear after careful choice of n , which is a parameter and part of the algorithm inputs. When linear kernel is used and $n = T^{\frac{d+1}{2}}$, we have $\mathbb{E}[R_T] = \tilde{O}(d\sqrt{T})$. Even when linear kernel is used and $K = T$, we have $\mathbb{E}[R_T] = \tilde{O}(d\sqrt{T} + \sqrt{dT}^{\frac{d}{d+1}})$ which is still a no-regret bound.*

Proof. Our proof starts from the bounding the error term incurred in the post-decoding process. Let S denote the set of n data points sampled *i.i.d.* from domain \mathcal{X} and ϵ denote the expected distance between any data point x and its nearest neighbor x' in \mathcal{X} , i.e.,

$$\epsilon = \mathbb{E}_{x, \mathcal{X}}[\|x - x'\|_2].$$

Recall that $\mathcal{X} \subseteq [0, 1]^d$ and we discretize it in each dimension using distance ϵ and we get $r = (1/\epsilon)^d$ small boxes. Each small box $C_i \forall i \in 1, \dots, r$ is a covering set of the domain. For any two data points in the same box we have $\|x_1 - x_2\| \leq \sqrt{d}\epsilon$, otherwise, $\|x_1 - x_2\| \leq \sqrt{d}$. Therefore,

$$\epsilon \leq \mathbb{E}_S \left[\mathbb{P} \left[\bigcup_{i: C_i \cap S = \emptyset} C_i \right] \sqrt{d} + \mathbb{P} \left[\bigcup_{i: C_i \cap S \neq \emptyset} C_i \right] \epsilon \sqrt{d} \right].$$

By Lemma 6 and $\mathbb{P}[\cup_{i: C_i \cap S \neq \emptyset} C_i] \leq 1$ we have

$$\begin{aligned} \epsilon &\leq \sqrt{d} \left(\frac{r}{ne} + \epsilon \right) \\ &= \sqrt{d} \left(\frac{(1/\epsilon)^d}{ne} + \epsilon \right) \\ &\leq 2\sqrt{d} n^{-\frac{1}{d+1}}, \end{aligned} \tag{2}$$

where the last step is by choosing $\epsilon = n^{-1/(d+1)}$.

By definition of expected cumulative regret,

$$\begin{aligned} \mathbb{E}[R_T] &= \mathbb{E} \left[\sum_{i=1}^T f(\hat{x}_t) - f(x_*) \right] \\ &= \mathbb{E} \left[\sum_{i=1}^T g(z_t) - g(z_*) \right] \\ &= \mathbb{E} \left[\sum_{i=1}^T g(\hat{z}_t) - g(z_*) + g(z_t) - g(\hat{z}_t) \right], \end{aligned}$$

where $\hat{z}_t = p(\hat{x}_t)$ is an auxiliary data point in \mathcal{Z} . We need it because new observation is queried at \hat{x}_t rather than x_t . To continue the proof, we use triangular inequality and Assumptions 1 and 2,

$$\begin{aligned} \mathbb{E}[R_T] &\leq \mathbb{E} \left[\sum_{i=1}^T g(\hat{z}_t) - g(z_*) \right] + O(\epsilon C_p C_g T) \\ &\leq \tilde{O}(\sqrt{T\gamma_T} + \epsilon C_p C_g T), \end{aligned}$$

where the last inequality is due to Lemma 5. The proof completes by plugging in eq. (2). \square

The proof above relies on following two lemmas.

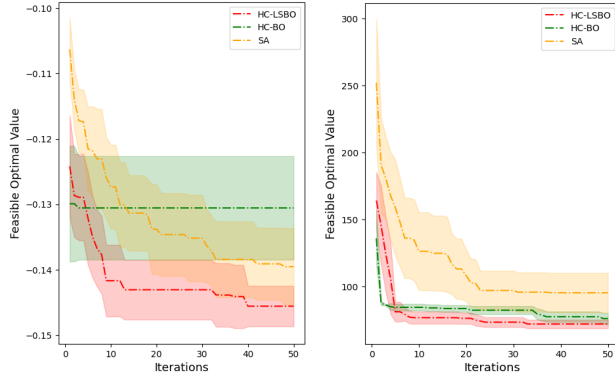
Lemma 5 (Regret bound of GP-LCB (Theorem 1 of [Srinivas et al., 2010])). *Let $\delta \in (0, 1)$ and $\beta_t = 2 \log(mt^2\pi^2/6\delta)$. Running GP-UCB with β_t for a sample f of a GP with mean function zero and covariance function $k(x, x')$, we obtain a regret bound of $\tilde{O}(\sqrt{T\gamma_T \log n})$ with high probability. Precisely,*

$$\mathbb{P}[R_T \geq \sqrt{C_1 T \beta_T \gamma_T} \forall T \geq 1] \geq 1 - \delta,$$

where $C_1 = 8/\log(1 + \delta^{-2})$.

Lemma 6 (Expected minimum distance (Lemma 19.2 of [Shalev-Shwartz and Ben-David, 2014])). *Let C_1, \dots, C_r be a collection of covering sets of some domain set \mathcal{X} . Let S be a sequence of n points sampled *i.i.d.* according to some probability distribution \mathcal{D} over \mathcal{X} . Then,*

$$\mathbb{E}_{S \sim \mathcal{D}^n} \left[\sum_{i \in C_i \cap S = \emptyset} \mathbb{P}(C_i) \right] \leq \frac{r}{ne}.$$



(a) Keane's bump function. (b) Levy function.

Figure 4: Comparisons of performance convergence with 95% confidence intervals for (a) 30-dimensional Keane's bump function and (b) 50-dimensional Levy function, respectively.

5 Experiments

We compare our HC-LSBO algorithm against three baseline approaches that can be used to address HCBBO problems. These baselines include (1) simulated annealing (SA) [Kirkpatrick et al., 1983], (2) approximated Mixed Integer Linear Programming (MILP) [Zhu et al., 2022], and (3) a variant of our algorithm without the latent decision model, referred to as Hidden-Constrained Bayesian Optimization (HC-BO), serving as an ablation comparison.

We train the latent decision model in our framework with the Adam optimizer [Kingma and Ba, 2015]. Both HC-BO and HC-LSBO are performed under the identical set of hyperparameters, providing an ablation comparison to assess the impact of the latent decision model in HC-LSBO. Each method is executed 10 times across all experiments to determine the 95% confidence interval of their results. Implementation details of these methods can be found in Appendix B.

Note that we only include MILP as a baseline method in the districting problems because the continuity and compactness in these problems can be expressed as a set of linear constraints, albeit with the trade-offs of adding auxiliary variables and incurring computational expenses. Nonetheless, in other scenarios, including our synthetic experiments, direct application of MILP is not feasible.

5.1 Synthetic results

We consider minimizing (a) the 30D Keane's bump function [Keane, 1994] and (b) the 50D Levy function [Laguna and Martí, 2005], both of which are common test functions for constrained optimization. To obtain samples from hidden constraints, the conundrum we aim to address via our methodology, we first gen-

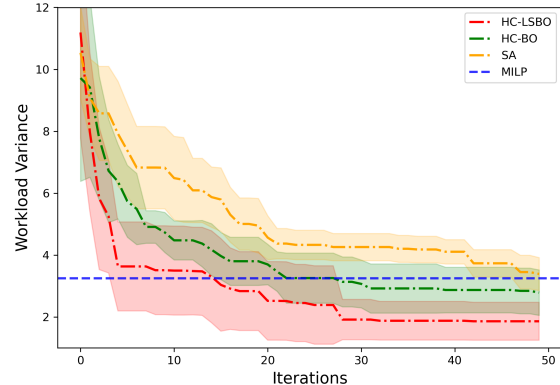


Figure 5: Performance convergence with a 95% confidence interval on the 6×6 grid districting problem.

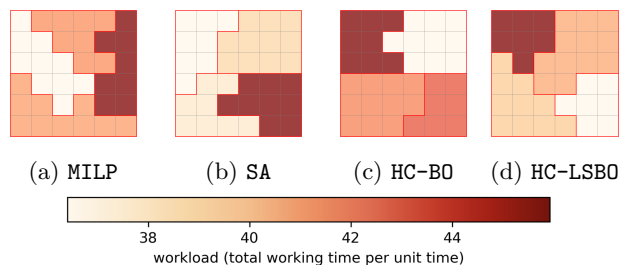


Figure 6: Districting plans for the 6×6 grid districting problem. The workloads are indicated by the depth of the color.

erate $n = 2,000$ samples from the standard uniform distribution in the 10D latent space and decode them through a randomly initialized decoder. In this way, the feasible regions remain unknown, while we are still allowed to draw feasible decision samples using the decoder. We scale the samples accordingly so that the test functions can be evaluated under their standard domains, *i.e.*, the Keane's bump function on $[0, 10]^d$ and the Levy function on $[-10, 10]^d$.

Figure 4 presents the synthetic results. It is evident that our method attains the lowest objective values consistently compared to other baseline methods. In Figure 4 (a), in particular, we observe that the integration of the latent decision model into HC-LSBO greatly enhances the BO's performance. This is in stark contrast to HC-BO, which doesn't yield satisfactory outcomes. See additional synthetic results in Appendix C.

5.2 Case study: Police redistricting

One common application of high-dimensional HCBBO in public policymaking is redistricting. For example, in police redistricting problems, the goal is to distribute L police service regions across J distinct zones. Each service region is patrolled by a single police unit. While units within the same zone can assist each other, assistance across different zones is disallowed. The objective is to minimize the workload variance across all the

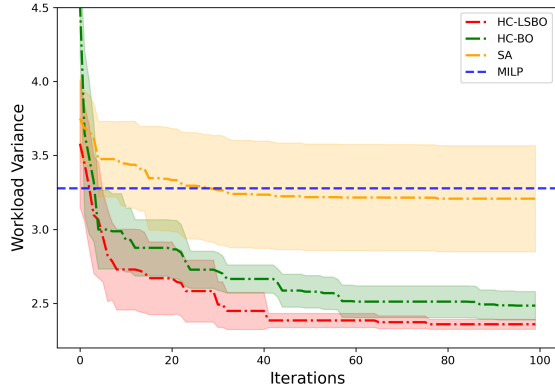


Figure 7: Performance convergence with a 95% confidence interval on the real police districting problem in Atlanta, Georgia.

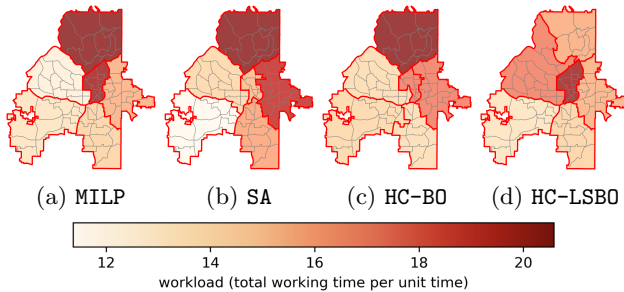


Figure 8: Districting plans for the real police districting problem in Atlanta, Georgia.

zones, which is assessed using the hypercube queuing models [Larson, 1974]. This model can be regarded as a costly black-box function. The decision variables are defined by the assignment of a region to a zone, represented by matrix $x \in \{0, 1\}^{L \times J}$. Here, an entry $x_{lj} = 1$ indicates region l is allocated to zone j , and $x_{lj} = 0$ otherwise. A primal constraint is that each region should be assigned to only one zone. This means that for every region l , $\sum_{j \in [J]} x_{lj} = 1$. There are also hidden constraints to consider. One such constraint is contiguity, which ensures that all regions within a specific zone are adjacent.

Redistricting 6×6 grid We first evaluate our algorithm using a synthetic scenario, consisting of a 6×6 grid to be divided into 4 zones, and the decision variable $x \in \{0, 1\}^{36 \times 4}$. For each region l , the arrival rate λ_l is independently drawn from a standard uniform distribution. Moreover, all regions share an identical service rate of $\mu = 1$. We generate an initial observation set X by simulating $n = 10,000$ feasible solutions.

Figure 5 demonstrates that our method notably surpasses other baseline methods regarding objective value and convergence speed. Additionally, in Figure 6, we show the optimal districting plans derived from our algorithm alongside those from the baseline methods. It is evident that our approach produces a more

balanced plan compared to the other methods.

Atlanta police redistricting For the police zone design in Atlanta, there are 78 police service regions that need to be divided into 6 zones, with the decision variable represented as $x \in \{0, 1\}^{78 \times 6}$. The redistricting of Atlanta’s police zones is constrained by several hidden factors. These include contiguity and compactness, as well as other practical constraints that cannot be explicitly defined. One such hidden constraint is the need for changes to the existing plan should be taken in certain local areas. A drastic design change is undesirable because: (1) A large-scale operational change will result in high implementation costs. (2) A radical design change will usually face significant uncertainties and unpredictable risks in future operations.

The arrival rate λ_l and the service rate μ are estimated using historical 911-calls-for-service data collected in the years 2021 and 2022 [Zhu and Xie, 2019, Zhu and Xie, 2022, Zhu et al., 2022]. We generate an initial observation set X by simulating $n = 10,000$ feasible solutions which are the neighbors of the existing plan with changes in certain local areas.

Figure 7 displays the convergence of our algorithm in comparison to other baseline methods, showing a consistent reduction in workload variance. As shown in Figure 8, the plan produced by our HC-LSBO algorithm achieves the lowest workload variance, surpassing both the HC-BO and SA algorithms. It’s worth highlighting the limitations of the HC-BO algorithm. Its inefficiency stems from the inadequacy of the Euclidean norm in the original decision space, especially when dealing with high dimensionality and complex feasible region structures.

6 Discussion

We introduce a new category of optimization problems termed Hidden-Constrained Black-Box Optimization (HCBBO), which poses challenges for conventional BO methods. To address this, we have developed the HC-LSBO algorithm by leveraging a set of observed feasible decisions. The core idea is to learn a latent representation of feasible decisions to effectively overcome the complications posed by hidden constraints. Our algorithm facilitates BO within an unconstrained and more compact decision space. Additionally, our method can also accommodate traditional constraints by first generating samples that satisfy these constraints and then employing our algorithm for optimization, which yields another potential use case for our framework. However, it is worth noting that our method’s efficacy hinges on the feasible decision samples adequately covering the feasible region. This dependency might restrict its broader application, particularly in situations where data is limited.

References

- [Antonova et al., 2020] Antonova, R., Rai, A., Li, T., and Kragic, D. (2020). Bayesian optimization in variational latent spaces with dynamic compression. In Kaelbling, L. P., Kragic, D., and Sugiura, K., editors, *Proceedings of the Conference on Robot Learning*, volume 100 of *Proceedings of Machine Learning Research*, pages 456–465. PMLR.
- [Ariafar et al., 2019] Ariafar, S., Coll-Font, J., Brooks, D., and Dy, J. (2019). Admmbo: Bayesian optimization with unknown constraints using admm. *Journal of Machine Learning Research*, 20(123):1–26.
- [Audet et al., 2020] Audet, C., Caporossi, G., and Jacquet, S. (2020). Binary, unrelaxable and hidden constraints in blackbox optimization. *Operations Research Letters*, 48(4):467–471.
- [Binois and Wycoff, 2022] Binois, M. and Wycoff, N. (2022). A survey on high-dimensional gaussian process modeling with application to bayesian optimization. *ACM Transactions on Evolutionary Learning and Optimization*, 2(2):1–26.
- [Chandak et al., 2020] Chandak, A., Dey, D., Mukhoty, B., and Kar, P. (2020). Epidemiologically and socio-economically optimal policies via bayesian optimization. *Transactions of the Indian National Academy of Engineering*, 5:117–127.
- [Char et al., 2019] Char, I., Chung, Y., Neiswanger, W., Kandasamy, K., Nelson, A. O., Boyer, M., Kolen, E., and Schneider, J. (2019). Offline contextual bayesian optimization. *Advances in Neural Information Processing Systems*, 32.
- [Chen et al., 2023] Chen, C., Beckham, C., Liu, Z., Liu, X., and Pal, C. (2023). Parallel-mentoring for offline model-based optimization. *arXiv preprint arXiv:2309.11592*.
- [Choi et al., 2000] Choi, T. D., Eslinger, O. J., Kelley, C. T., David, J. W., and Etheridge, M. (2000). Optimization of automotive valve train components with implicit filtering. *Optimization and Engineering*, 1:9–27.
- [Dai et al., 2022] Dai, Z., Shu, Y., Low, B. K. H., and Jaillet, P. (2022). Sample-then-optimize batch neural thompson sampling. *Advances in Neural Information Processing Systems*, 35:23331–23344.
- [Deshwal and Doppa, 2021] Deshwal, A. and Doppa, J. (2021). Combining latent space and structured kernels for bayesian optimization over combinatorial spaces. *Advances in Neural Information Processing Systems*, 34:8185–8200.
- [Doersch, 2016] Doersch, C. (2016). Tutorial on variational autoencoders. *arXiv preprint arXiv:1606.05908*.
- [Eissman et al., 2018] Eissman, S., Levy, D., Shu, R., Bartzsch, S., and Ermon, S. (2018). Bayesian optimization and attribute adjustment. In *Proc. 34th Conference on Uncertainty in Artificial Intelligence*.
- [Eriksson and Poloczek, 2021] Eriksson, D. and Poloczek, M. (2021). Scalable constrained bayesian optimization. In Banerjee, A. and Fukumizu, K., editors, *Proceedings of The 24th International Conference on Artificial Intelligence and Statistics*, volume 130 of *Proceedings of Machine Learning Research*, pages 730–738. PMLR.
- [Gardner et al., 2014] Gardner, J. R., Kusner, M. J., Xu, Z. E., Weinberger, K. Q., and Cunningham, J. P. (2014). Bayesian optimization with inequality constraints. In *ICML*, volume 2014, pages 937–945.
- [Gelbart et al., 2014] Gelbart, M. A., Snoek, J., and Adams, R. P. (2014). Bayesian optimization with unknown constraints. UAI’14. AUAI Press.
- [Guo et al., 2023] Guo, J., Ranković, B., and Schwaller, P. (2023). Bayesian optimization for chemical reactions. *Chimia*, 77(1/2):31–31.
- [Jordan et al., 1999] Jordan, M. I., Ghahramani, Z., Jaakkola, T. S., and Saul, L. K. (1999). An introduction to variational methods for graphical models. *Machine learning*, 37:183–233.
- [Kandasamy et al., 2020] Kandasamy, K., Vysyaraju, K. R., Neiswanger, W., Paria, B., Collins, C. R., Schneider, J., Póczos, B., and Xing, E. P. (2020). Tuning hyperparameters without grad students: Scalable and robust bayesian optimisation with dragonfly. *The Journal of Machine Learning Research*, 21(1):3098–3124.
- [Keane, 1994] Keane, A. (1994). Experiences with optimizers in structural design. In *In Proceedings of the conference on adaptive computing in engineering design and control*, volume 94, pages 14–27.
- [Kingma and Ba, 2015] Kingma, D. and Ba, J. (2015). Adam: A method for stochastic optimization. In *International Conference on Learning Representations (ICLR)*, San Diego, CA, USA.
- [Kirkpatrick et al., 1983] Kirkpatrick, S., Gelatt Jr, C. D., and Vecchi, M. P. (1983). Optimization by simulated annealing. *science*, 220(4598):671–680.
- [Krishnamoorthy et al., 2023] Krishnamoorthy, S., Mashkaria, S. M., and Grover, A. (2023). Diffusion models for black-box optimization. *arXiv preprint arXiv:2306.07180*.

-
- [Laguna and Martí, 2005] Laguna, M. and Martí, R. (2005). Experimental testing of advanced scatter search designs for global optimization of multimodal functions. *Journal of Global Optimization*, 33:235–255.
- [Larson, 1974] Larson, R. C. (1974). A hypercube queuing model for facility location and redistricting in urban emergency services. *Computers & Operations Research*, 1(1):67–95.
- [Larson and Odoni, 1981] Larson, R. C. and Odoni, A. R. (1981). *Urban operations research*. Number Monograph.
- [Letham et al., 2019] Letham, B., Karrer, B., Ottoni, G., and Bakshy, E. (2019). Constrained Bayesian Optimization with Noisy Experiments. *Bayesian Analysis*, 14(2):495 – 519.
- [Liu and Wang, 2023] Liu, C. and Wang, Y.-X. (2023). Global optimization with parametric function approximation. In *International Conference on Machine Learning*, pages 22113–22136. PMLR.
- [Luong et al., 2019] Luong, P., Gupta, S., Nguyen, D., Rana, S., and Venkatesh, S. (2019). Bayesian optimization with discrete variables. In *AI 2019: Advances in Artificial Intelligence: 32nd Australasian Joint Conference, Adelaide, SA, Australia, December 2–5, 2019, Proceedings 32*, pages 473–484. Springer.
- [Maus et al., 2022] Maus, N., Jones, H., Moore, J., Kusner, M. J., Bradshaw, J., and Gardner, J. (2022). Local latent space bayesian optimization over structured inputs. *Advances in Neural Information Processing Systems*, 35:34505–34518.
- [Pinheiro Cinelli et al., 2021] Pinheiro Cinelli, L., Araújo Marins, M., Barros da Silva, E. A., and Lima Netto, S. (2021). Variational autoencoder. In *Variational Methods for Machine Learning with Applications to Deep Networks*, pages 111–149. Springer.
- [Seeger, 2004] Seeger, M. (2004). Gaussian processes for machine learning. *International journal of neural systems*, 14(02):69–106.
- [Shahriari et al., 2015] Shahriari, B., Swersky, K., Wang, Z., Adams, R. P., and De Freitas, N. (2015). Taking the human out of the loop: A review of bayesian optimization. *Proceedings of the IEEE*, 104(1):148–175.
- [Shalev-Shwartz and Ben-David, 2014] Shalev-Shwartz, S. and Ben-David, S. (2014). *Understanding machine learning: From theory to algorithms*. Cambridge university press.
- [Shirabe, 2009] Shirabe, T. (2009). Districting modeling with exact contiguity constraints. *Environment and Planning B: Planning and Design*, 36(6):1053–1066.
- [Srinivas et al., 2010] Srinivas, N., Krause, A., Kakade, S., and Seeger, M. (2010). Gaussian process optimization in the bandit setting: No regret and experimental design. In *Proceedings of the 27th International Conference on Machine Learning*, pages 1015–1022.
- [Srinivas et al., 2009] Srinivas, N., Krause, A., Kakade, S. M., and Seeger, M. (2009). Gaussian process optimization in the bandit setting: No regret and experimental design. *arXiv preprint arXiv:0912.3995*.
- [Turner et al., 2021] Turner, R., Eriksson, D., McCourt, M., Kiili, J., Laaksonen, E., Xu, Z., and Guyon, I. (2021). Bayesian optimization is superior to random search for machine learning hyperparameter tuning: Analysis of the black-box optimization challenge 2020. In *NeurIPS 2020 Competition and Demonstration Track*, pages 3–26. PMLR.
- [Ueno et al., 2016] Ueno, T., Rhone, T. D., Hou, Z., Mizoguchi, T., and Tsuda, K. (2016). Combo: An efficient bayesian optimization library for materials science. *Materials discovery*, 4:18–21.
- [van Veenstra and Kotterink, 2017] van Veenstra, A. F. and Kotterink, B. (2017). Data-driven policy making: The policy lab approach. In *Electronic Participation: 9th IFIP WG 8.5 International Conference, ePart 2017, St. Petersburg, Russia, September 4-7, 2017, Proceedings 9*, pages 100–111. Springer.
- [Varol et al., 2012] Varol, A., Salzmann, M., Fua, P., and Urtasun, R. (2012). A constrained latent variable model. In *2012 IEEE conference on computer vision and pattern recognition*, pages 2248–2255. Ieee.
- [Wan et al., 2021] Wan, X., Nguyen, V., Ha, H., Ru, B., Lu, C., and Osborne, M. A. (2021). Think global and act local: Bayesian optimisation over high-dimensional categorical and mixed search spaces. *arXiv preprint arXiv:2102.07188*.
- [Williams and Rasmussen, 2006] Williams, C. K. and Rasmussen, C. E. (2006). *Gaussian processes for machine learning*, volume 2. MIT press Cambridge, MA.
- [Xie et al., 2021] Xie, W., Nie, W., Saffari, P., Robledo, L. F., Descote, P.-Y., and Jian, W. (2021). Landslide hazard assessment based on bayesian

optimization–support vector machine in nanping city, china. *Natural Hazards*, 109(1):931–948.

[Xing and Hua, 2022] Xing, W. and Hua, C. (2022). Optimal unit locations in emergency service systems with bayesian optimization. In *INFORMS International Conference on Service Science*, pages 439–452. Springer.

[Yu et al., 2021] Yu, S., Qing, Q., Zhang, C., Shehzad, A., Oatley, G., and Xia, F. (2021). Data-driven decision-making in covid-19 response: A survey. *IEEE Transactions on Computational Social Systems*, 8(4):1016–1029.

[Zhang et al., 2020] Zhang, Y., Apley, D. W., and Chen, W. (2020). Bayesian optimization for materials design with mixed quantitative and qualitative variables. *Scientific reports*, 10(1):4924.

[Zhu et al., 2020] Zhu, S., Bukharin, A. W., Lu, L., Wang, H., and Xie, Y. (2020). Data-driven optimization for police beat design in south fulton, georgia. *arXiv preprint arXiv:2004.09660*.

[Zhu et al., 2022] Zhu, S., Wang, H., and Xie, Y. (2022). Data-driven optimization for atlanta police-zone design. *INFORMS Journal on Applied Analytics*, 52(5):412–432.

[Zhu and Xie, 2019] Zhu, S. and Xie, Y. (2019). Crime event embedding with unsupervised feature selection. In *ICASSP 2019-2019 IEEE International Conference on Acoustics, Speech and Signal Processing (ICASSP)*, pages 3922–3926. IEEE.

[Zhu and Xie, 2022] Zhu, S. and Xie, Y. (2022). Spatiotemporal-textual point processes for crime linkage detection. *The Annals of Applied Statistics*, 16(2):1151–1170.

A Implementation details of the latent decision model

Here we present the derivation of the the evidence lower bound of the log-likelihood in Eq (1).

Given observation x and the latent random variable z , let $p(x)$ denote the likelihood of x , and $p(x|z)$ denote the conditional distribution of x given latent variable z . Let $\varphi(z)$ denote the prior distribution of the latent random variable z , and $q(z|x)$ denote the posterior distribution of z after observing x . The likelihood of observation x can be written as:

$$p(x) = \int p(x, z) dz = \mathbb{E}_{q(z|x)} \left[\frac{p(x, z)}{q(z|x)} \right]$$

By taking the logarithm on both sides and then applying Jensen’s inequality, we can get the lower bound of the log-likelihood $\mathcal{L}_{\text{ELBO}}(x)$ as follows:

$$\begin{aligned} \log p(x) &= \log \mathbb{E}_{q(z|x)} \left[\frac{p(x, z)}{q(z|x)} \right] \\ &\geq \mathbb{E}_{q(z|x)} \left[\log \frac{p(x, z)}{q(z|x)} \right] \\ &= \mathbb{E}_{q(z|x)} \left[\log \frac{p(x|z)\varphi(z)}{q(z|x)} \right] \\ &= \mathbb{E}_{q(z|x)} [\log p(x|z)] + \mathbb{E}_{q(z|x)} \left[\log \frac{\varphi(z)}{q(z|x)} \right] \\ &= \mathbb{E}_{q(z|x)} [\log p(x|z)] - \text{D}_{\text{KL}}(q(z|x) \parallel \varphi(z)) \end{aligned}$$

In practice, we add a hyperparameter η on the second term to modulate the penalization ratio.

$$\mathcal{L}_{\text{ELBO}}(x) = \mathbb{E}_{q(z|x)} [\log p(x|z)] - \eta \text{D}_{\text{KL}}(q(z|x) \parallel \varphi(z))$$

B Details of experimental setup

Experiments were conducted on a PC equipped with M1 Pro CPU and 16 GB RAM.

Synthetic experiments HC-LSBO 1,000 epoches with the learning rate of 10^{-4} , batch size 50, and $\eta = 0.1$ and dimension of latent space $d' = 10$. Both HC-B0 and HC-LSBO are performed under the identical set of hyperparameters: 10 initial evaluation points, $\beta = 1$ for the LCB, $M = 1,000$, and $T = 50$.

Redistricting experiments HC-LSBO 1,000 epoches with the learning rate of 10^{-3} , batch size 50 $\eta = 0.1$, and dimension of latent space $d' = 25$. Both HC-B0 and HC-LSBO are performed under the identical set of hyperparameters: 5 initial evaluation points, $\beta = 1$ for the LCB, $M = 10,000$, $T = 50$ (6×6 grid) and $T = 100$ (Atlanta).

The objective of the redistricting experiments is to minimize the workload variance across all the districts. The workload for each district j , denoted as ρ_j , is computed using the following equation:

$$\rho_j = (\tau_j + 1/\mu)\lambda_j$$

In this equation, τ_j represents the average travel time within district j , which can be estimated using the hypercube queuing model [Larson, 1974]. Recall that μ is the service rate for all districts and λ_j is the arrival rate in district j . Essentially, ρ_j quantifies the cumulative working duration per unit time for police units in district j . For clarity, a value of $\rho_j = 10$ implies that the combined working time of all police units in district j counts to 10 hours or minutes in every given hour or minute.

Algorithm 2: HC-BO

Input: Feasible decisions X ; Objective function \hat{f} ; Hyper-parameters m, T .
Randomly select $X_0 \subseteq X$;
Evaluate $Y_0 = \{\hat{f}(x) \mid x \in X_0\}$;
for $t \leftarrow 1$ **to** T **do**
 Train GP($\mu, k; \mathcal{X}$) using (X_{t-1}, Y_{t-1}) ;
 $\hat{X} \subseteq \mathcal{X}$; // Sample m decisions
 $x_t = \operatorname{argmin}_{x \in \hat{X}} \text{LCB}(x, \text{GP})$;
 $\hat{x}_t \leftarrow \phi(x_t)$; // Post-decoding
 $X_t \leftarrow X_{t-1} \cup \{\hat{x}_t\}$;
 $Y_t \leftarrow Y_{t-1} \cup \{\hat{f}(\hat{x}_t)\}$;
end
return $x^* = \operatorname{argmin}_{x \in X_T} \hat{f}(x)$

Algorithm 3: SA

Input: Objective function \hat{f} ; Initial solution x ; Hyper-parameters $\alpha = 0.8, C_{init} = 1, T$.
 $x^* \leftarrow x, t \leftarrow 0, C \leftarrow C_{init}$;
while $t < T$ **do**
 $x' \leftarrow \text{Neighbour}(x)$; // Randomly pick a neighbour
 $\Delta \leftarrow \hat{f}(x') - \hat{f}(x)$;
 $r \leftarrow$ draw uniformly from $[0, 1]$;
 if $\Delta < 0$ **or** $r < \exp(-\Delta/C)$ **then**
 $x \leftarrow x'$;
 end
 if $\hat{f}(x') < \hat{f}(x^*)$ **then**
 $x^* \leftarrow x'$;
 end
 $C \leftarrow \alpha C, t \leftarrow t + 1$; // Cooling temperature
end
return x^*

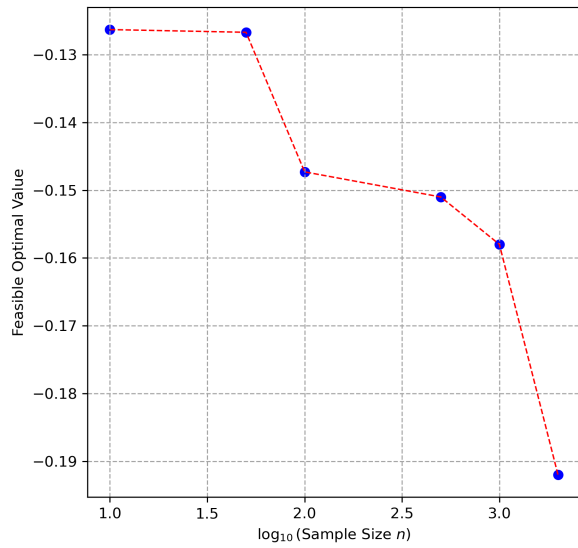
Baseline settings

1. HC-BO: Please refer to Algorithm 2.
2. Simulated Annealing: Please refer to Algorithm 3.
3. MILP: Please refer to Section E.3 in the Appendix of [Zhu et al., 2022].

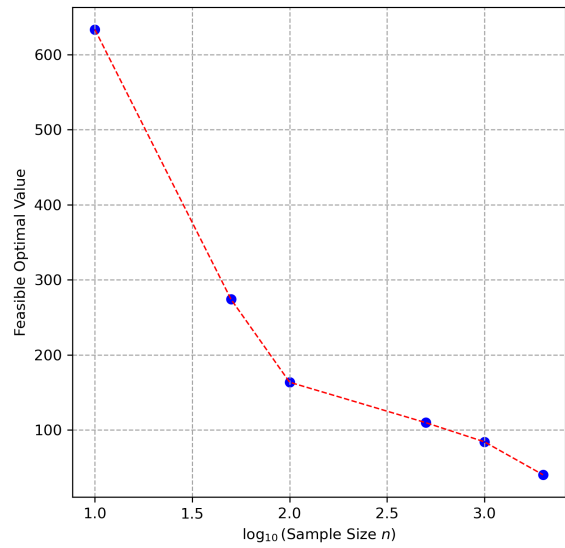
C Additional results

We conduct the sensitivity tests of our HC-LSBO algorithm with respect to the sample size n on both synthetic experiments and the real police redistricting problems in the 6×6 grid and Atlanta, Georgia.

In Figure 9 and Figure 10, we can observe that as the sample size n increases, our algorithm will obtain better decisions on both synthetic experiments and the real police redistricting problems. Note that the improvement reaches saturation when $n = 5000$ on the police redistricting problem in the 6×6 grid. The performance improvement is roughly in a logarithmic relationship with the growth of the sample size n .

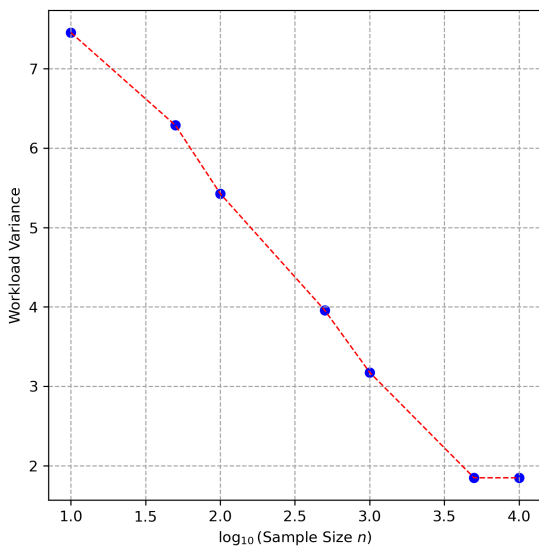


(a) Keane's bump function.

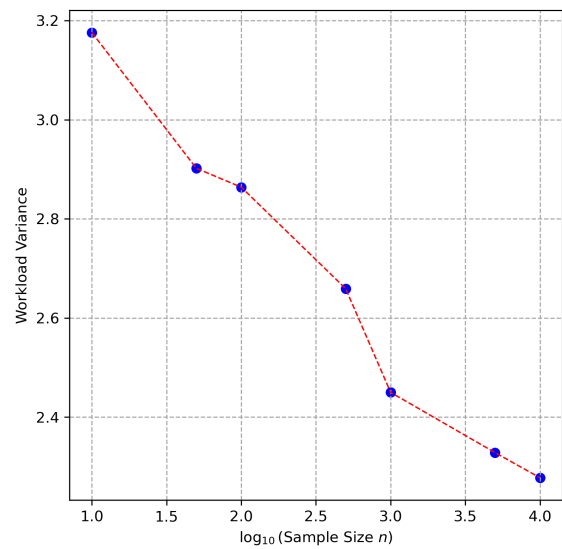


(b) Levy function.

Figure 9: Feasible optimal values obtained by HC-LSBO with various sample sizes on (a) the 30-dimensional Keane function and (b) the 50-dimensional Levy function. The x-axis represents the logarithm (base 10) of the sample size n .



(a) 6×6 grid.



(b) Atlanta.

Figure 10: Workload variance obtained by HC-LSBO with various sample sizes on the real police districting problem in (a) 6×6 grid and (b) Atlanta. The x-axis represents the logarithm (base 10) of the sample size n .